

Mathematical modeling and numerical computation of narrow escape problems

Alexei F. Cheviakov* and Ashton S. Reimer

Department of Mathematics and Statistics, University of Saskatchewan, Saskatoon, Canada S7N 5E6

Michael J. Ward†

Department of Mathematics, University of British Columbia, Vancouver, Canada V6T 1Z2

(Received 24 February 2011; revised manuscript received 12 December 2011; published 22 February 2012)

The narrow escape problem refers to the problem of calculating the mean first passage time (MFPT) needed for an average Brownian particle to leave a domain with an insulating boundary containing N small well-separated absorbing windows, or traps. This mean first passage time satisfies the Poisson partial differential equation subject to a mixed Dirichlet-Neumann boundary condition on the domain boundary, with the Dirichlet condition corresponding to absorbing traps. In the limit of small total trap size, a common asymptotic theory is presented to calculate the MFPT in two-dimensional domains and in the unit sphere. The asymptotic MFPT formulas depend on mutual trap locations, allowing for global optimization of trap locations. Although the asymptotic theory for the MFPT was developed in the limit of asymptotically small trap radii, and under the assumption that the traps are well-separated, a comprehensive study involving comparison with full numerical simulations shows that the full numerical and asymptotic results for the MFPT are within 1% accuracy even when total trap size is only moderately small, and for traps that may be rather close together. This close agreement between asymptotic and numerical results at finite, and not necessarily asymptotically small, values of the trap size clearly illustrates one of the key side benefits of a theory based on a systematic asymptotic analysis. In addition, for the unit sphere, numerical results are given for the optimal configuration of a collection of traps on the surface of a sphere that minimizes the average MFPT. The case of N identical traps and a pattern of traps with two different sizes are considered. The effect of trap fragmentation on the average MFPT is also discussed.

DOI: [10.1103/PhysRevE.85.021131](https://doi.org/10.1103/PhysRevE.85.021131)

PACS number(s): 05.40.Jc, 02.30.Jr, 02.30.Mv, 02.60.Lj

I. INTRODUCTION

Narrow escape problems are ubiquitous in biological modeling, since they arise naturally in the description of Brownian particles that attempt to escape from a bounded domain through small absorbing windows on an otherwise reflecting boundary. In the biological context, the Brownian particles could be diffusing ions, globular proteins, or cell-surface receptors. It is then of interest to determine, for example, the mean time that an ion requires to find an open channel located in the cell membrane or the mean time for a receptor to hit a certain target binding site (cf. [1–4]). Similar problems also arise in the modeling of escape kinetics in chemistry [5].

Consider the trajectory $X(t)$ of a Brownian particle confined in a bounded domain $\Omega \in \mathbb{R}^d$, $d = 2, 3$, for which the boundary $\partial\Omega$ is almost entirely reflecting except for small windows (traps) centered at the points $x_j \in \partial\Omega$, for $j = 1, \dots, N$, through which the particle can escape (see Fig. 1).

The mean first passage time (MFPT) $v(x)$ is defined as the expectation value of the time taken for the Brownian particle starting initially from $X(0) = x \in \Omega$ to become absorbed by one of the boundary traps. It is well known that, in the continuum limit, the MFPT $v(x)$ satisfies the mixed Dirichlet-Neumann problem (cf. [3]),

$$\begin{aligned} \Delta v &= -\frac{1}{D}, \quad x \in \Omega; \quad \partial_n v = 0, \quad x \in \partial\Omega_r, \\ v &= 0, \quad x \in \partial\Omega_a = \bigcup_{j=1}^N \partial\Omega_{\varepsilon_j}, \end{aligned} \quad (1.1)$$

where D is the constant diffusivity. For two- and three-dimensional problems with $\text{diam}(\Omega) = O(1)$, the windows Ω_{ε_j} are respectively characterized by a length $|\partial\Omega_{\varepsilon_j}| = O(\varepsilon)$ or an area $|\partial\Omega_{\varepsilon_j}| = O(\varepsilon^2)$, where $\varepsilon \ll 1$ is a small parameter.

Due to the mixed nature of the boundary condition for the partial differential equation (PDE) (1.1), no exact and only a few approximate solutions are known for an arbitrary-shaped domain. In particular, leading-order terms for the asymptotic expansion of the MFPT in the limit $\varepsilon \rightarrow 0$ have been recently derived for a unit disk with one and two traps [6,7], a two-dimensional domain with a single trap located at a cusp of a boundary [8], and a unit sphere and a general three-dimensional domain with smooth boundary and with a single trap [9,10]. A recent survey of the calculation of the MFPT for small targets in the interior or on the boundary of a confining domain is given in [11].

The method of matched asymptotic expansions was used to derive new asymptotic MFPT formulas in the limit $\varepsilon \rightarrow 0$ for two-dimensional (2D) [12] and three-dimensional (3D) [13] domains with an arbitrary number of nonidentical, but well-separated, boundary traps. In Sec. II, we present the asymptotic formulas for two-dimensional and three-dimensional domains in a common general framework. These formulas employ the Neumann Green's function for each respective domain, and can be used for direct computations for domains for which this Green's function is known analytically. Such domains include the unit square, the unit disk, or the unit sphere. Importantly, the formulas for the average MFPT include an additional term, called the *interaction energy*, which depends on the mutual positions of the traps. This leads naturally to certain discrete variational problems whereby the average MFPT is to be minimized with respect to the trap locations. Recently, in [14],

*Corresponding author: chevaikov@math.usask.ca

†ward@math.ubc.ca

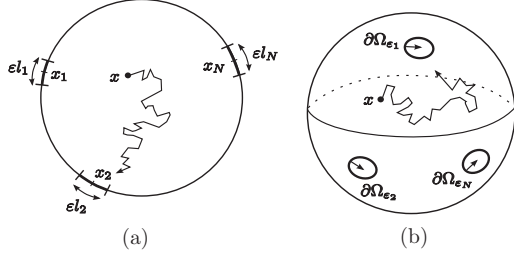


FIG. 1. Schematic of the narrow escape problem in a 2D and 3D domain.

a rigorous proof of some of the asymptotic results in [12,13] has been given.

Section II also discusses specific forms of asymptotic MFPT formulas relevant for the unit disk, the unit square, and the unit sphere. In particular, for the case of N identical traps on a unit sphere, the traps “repel” in an analogous way to the physical situation of N electrons bound to a sphere. The interaction energy for our pattern of traps is a combination of a Coulombic energy, a logarithmic energy, and an additional logarithmic term. The corresponding global optimization problem that minimizes the combined interaction energy, and thus the average MFPT, has been discussed in [13] and the results have been compared with many recent results on the global optimization of the interaction energy of point particles on the sphere that interact through either purely Coulomb or logarithmic forces (see [15–19]). An expression for a new interaction energy for a pattern of $2N$ traps, which consists of N small traps of a common radius and N large traps of a common radius, is also derived in Sec. II.

In Sec. III, the relation is examined between the average MFPT result for an equally spaced arrangement of identical boundary traps for a unit disk and the corresponding result that can be obtained from the dilute fraction limit of homogenization theory [20], where the mixed Dirichlet-Neumann boundary condition of the problem (1.1) is replaced by an effective Robin boundary condition.

The common feature of all formal asymptotic results is the unknown behavior of higher-order (error) terms and, hence, the applicability limits of the asymptotic theory. In Sec. IV, this issue is studied by comparing asymptotic results for the MFPT and the average MFPT for the unit disk, unit square, and the unit sphere, with full numerical computations obtained by solving the underlying PDE (1.1) numerically. For each of these special domains, the Neumann Green’s function required to evaluate the terms in the asymptotic expansions of the MFPT is known analytically. Although the asymptotic theory of [12,13] for the MFPT was developed in the limit of asymptotically small trap radii, and under the assumption that the traps are well-separated, in Sec. IV, we show upon comparison with full numerical results that the asymptotic results reliably predict the MFPT to within 1% accuracy when ε is only moderately small and for traps that may be rather close to each other. This close agreement between asymptotic and numerical results at finite, and not necessarily asymptotically small, values of the trap size ε illustrates one of the often key benefits of a systematic asymptotic analysis. The quality of the approximation afforded by the asymptotic MFPT solution in

the vicinity of a trap is examined through the comparison with numerical results in Sec. IV C.

Another goal of this paper is to compute some optimal arrangements of traps on the surface of the unit sphere. The problem of the global optimization of the locations of surface-bound particles interacting under various types of forces has been actively studied (cf. [15–19]). In the context of the narrow escape problem, the third term in the asymptotic expansion as $\varepsilon \rightarrow 0$ of the average MFPT depends on the global configuration of traps on the surface of the sphere. The associated problem of minimizing the average MFPT leads to a new class of weighted discrete variational problems with an interaction energy that has not been studied in the classical works of [15–19]. In Sec. V, we present optimization results for the new interaction energy for a pattern of N identical traps and for a pattern of $2N$ traps, which consists of N small traps of a common radius and N large traps of a common radius. By using scaling laws valid for large N for the minimal-energy configurations, trap fragmentation effects on the average MFPT are studied.

II. ASYMPTOTIC FORMULAS FOR THE MEAN FIRST PASSAGE TIMES

The current section outlines the method of matched asymptotic expansions to calculate the asymptotic MFPT $v(x)$ for the narrow escape problem in two- and three-dimensional domains. The corresponding asymptotic formulas for the MFPT and the average MFPT are given in general, as well as for some specific domains. For specific details, see [12,13].

Consider a small trap centered at a point x_j on the domain boundary. In terms of the local coordinate $y = \varepsilon^{-1}(x - x_j)$, the expansion of the inner solution near this j th trap has the form

$$v(x) \equiv w(y) = w_0 + w_1 + w_2 + \dots, \quad (2.1)$$

where w_q for $q = 0, 1, \dots$ are proportional to either powers of ε or terms of the form $\varepsilon^p \log \varepsilon$, $p \in \mathbb{Z}$, starting from an appropriate term. In particular, for $\Omega \in \mathbb{R}^3$, $w_0 = O(\varepsilon^{-1})$, $w_1 = O(\log \varepsilon)$, $w_2 = O(\varepsilon^0)$, etc. For domains in \mathbb{R}^2 , $w_0 = O(\log \varepsilon)$, $w_1 = O(\varepsilon^0)$, $w_2 = O(-1/\log \varepsilon)$, etc.

In the outer region, defined at $O(1)$ distances from the traps, the outer expansion has the form

$$v(x) = v_0 + v_1 + v_2 + \dots \quad (2.2)$$

Then the two expansions are substituted into the PDE (1.1) and, upon equating comparable terms in ε , linear boundary value problems for v_q and w_q , $q = 0, 1, \dots$ are obtained. Finally, unknown constants in the functions v_q and w_q are determined in a systematic manner by imposing the matching condition that

$$v_0(x) + v_1(x) + \dots \sim w_0(y) + w_1(y) + \dots$$

In this condition, the left- and right-hand sides of this expression must agree as $x \rightarrow x_j$ and as $y = \varepsilon^{-1}(x - x_j) \rightarrow \infty$, respectively.

A key feature in the analysis is that the solution to the outer problems for the correction terms v_q for $q \geq 1$ involves the Neumann Green’s function $G(x; x_j)$ for the domain Ω with a

singularity at $x_j \in \partial\Omega$. This Green's function $G(x; \xi)$ is the unique solution of

$$\begin{aligned} \Delta G &= \frac{1}{|\Omega|}, \quad x \in \Omega; \quad \partial_n G = 0, \quad x \in \partial\Omega \setminus \{\xi\}; \\ \int_{\Omega} G dx &= 0, \end{aligned} \quad (2.3)$$

which has the following singularity behavior as $x \rightarrow \xi$ in either a two- or three-dimensional domain with smooth boundary:

$$\begin{aligned} G(x; \xi) &= -\frac{1}{\pi} \log|x - \xi| + R(\xi; \xi) \quad (2D), \\ G(x; \xi) &= \frac{1}{2\pi|x - \xi|} - \frac{\mathcal{H}_m}{4\pi} \log|x - \xi| + R(\xi; \xi) \quad (3D). \end{aligned} \quad (2.4)$$

In Eq. (2.3), ∂_n is the normal derivative to $\partial\Omega$, and $|\Omega|$ is the measure (area in \mathbb{R}^2 and volume in \mathbb{R}^3) of Ω . Here $\mathcal{H}_m = \mathcal{H}_m(\xi)$ is the mean curvature of the boundary at $\xi \in \partial\Omega$, with $\mathcal{H}_m = 1$ for the unit sphere, and $R(\xi; \xi)$ is the (bounded) regular part of the Green's function at the singularity.

The following general result characterizes the first correction term in the outer region for the MFPT $v(x)$ in terms of the Neumann Green's function, and holds for both two-dimensional and three-dimensional domains.

Principal result (2.1). In terms of the Neumann Green's function, the MFPT in a domain with N well-separated boundary traps centered at $x_j \in \partial\Omega$, for $j = 1, \dots, N$, is given asymptotically for $\varepsilon \rightarrow 0$ in the outer region $|x - x_j| \gg \varepsilon$ by

$$v(x) = \bar{v} + \sum_{j=1}^N k_j G(x; x_j) + O(\mathcal{E}), \quad (2.5)$$

where k_j for $j = 1, \dots, N$ are certain constants depending on ε that are found upon matching the inner and outer expansions, and \mathcal{E} is an error estimate also depending in ε . In Eq. (2.5), \bar{v} is the average MFPT given by

$$\bar{v} = \frac{1}{|\Omega|} \int_{\Omega} v(x) dx. \quad (2.6)$$

Particular forms of the expressions for k_j and \bar{v} depend on the trap sizes, the arrangement of the traps on the domain boundary, and the domain shape, as described below. The asymptotic order for the error estimate $O(\mathcal{E})$ for Eq. (2.5) will also be discussed.

A. Two-dimensional domains

Let $\Omega \subset \mathbb{R}^2$ be a domain with a smooth boundary. Suppose that N surface traps of length εl_j are centered at x_j for $j = 1, \dots, N$ [cf. Fig. 1(a)]. We define the logarithmic capacitance d_j and the gauge function $\mu_j = \mu_j(\varepsilon)$ by

$$d_j = \frac{l_j}{4}, \quad \mu_j = -\frac{1}{\log(\varepsilon d_j)}. \quad (2.7)$$

Define the diagonal matrix \mathcal{M} and the symmetric Green's matrix \mathcal{G} by

$$\mathcal{M} = \text{diag}(\mu_1, \dots, \mu_N), \quad \mathcal{G} \equiv \begin{pmatrix} R_1 & G_{12} & \cdots & G_{1N} \\ G_{21} & R_2 & \cdots & G_{2N} \\ \vdots & \vdots & \ddots & \vdots \\ G_{N1} & \cdots & G_{N,N-1} & R_N \end{pmatrix},$$

where $G_{ij} \equiv G(x_i; x_j)$, and $R_i \equiv R(x_i; x_i)$ is the self-interaction term. Also define the vector $e = (1, \dots, 1)^T$ and the matrix $E = ee^T/N$.

As shown in [12] an asymptotic expansion for the MFPT that accounts for all logarithmic terms in powers of μ_j is given by Eq. (2.5) with $k_j = -\pi A_j$, where the vector $A = (A_1, \dots, A_N)^T$ is the solution of the linear system,

$$\left[I + \pi \mathcal{M} \left(I - \frac{1}{\bar{\mu}} E \mathcal{M} \right) \mathcal{G} \right] A = \frac{|\Omega|}{D\pi N \bar{\mu}}. \quad (2.8)$$

In Eq. (2.8), $\bar{\mu} = (1/N) \sum_{j=1}^N \mu_j$. The average MFPT (2.6) is given by

$$\bar{v} = \frac{|\Omega|}{D\pi N \bar{\mu}} + \frac{\pi}{N \bar{\mu}} e^T \mathcal{M} \mathcal{G} A. \quad (2.9)$$

A rigorous proof of this result has recently been given in [14], together with the error estimate $O(\mathcal{E}) = O(\varepsilon)$.

The formulas above can be adapted to the case where the traps are not well-separated [12]. In particular, for a cluster of two absorbing windows of a common length εl_j with edge separation distance $2\varepsilon a_j$, both windows can be replaced by one effective window with the logarithmic capacitance d_j given by [see Eq. (2.19) of [12]]

$$d_j = \frac{l_j}{2} \left(1 + \frac{2a_j}{l_j} \right)^{1/2}. \quad (2.10)$$

This formula for d_j , pertaining to a cluster of two traps, is to replace the formula (2.7) of an individual trap. The formulas above can be adapted to the case where the traps are not well-separated by considering trap cluster capacitances d_j , and also to domains with piecewise-smooth boundaries [12].

Explicit formulas for the Neumann Green's function are known for the special cases when Ω is a unit disk or a unit square. We now summarize these results.

1. The unit disk

When Ω is the unit disk centered at the origin, the Neumann Green's function and its regular part are given explicitly by [21]

$$\begin{aligned} G(x; x_i) &= -\frac{1}{\pi} \log|x - x_i| + \frac{|x|^2}{4\pi} - \frac{1}{8\pi}, \\ R(x_i; x_i) &= \frac{1}{8\pi}, \quad |x_i| = 1. \end{aligned} \quad (2.11)$$

In the particular case of N absorbing arcs having a common length $|\partial\Omega_j| = 2\varepsilon$, a two-term asymptotic result for the average MFPT, obtained by approximating the infinite-logarithmic sum result from Eq. (2.9), is

$$\bar{v} \sim \frac{1}{DN} \left[-\log \frac{\varepsilon}{2} + \frac{N}{8} - \frac{1}{N} \sum_{i=1}^N \sum_{j=i+1}^N \log|x_i - x_j| \right]. \quad (2.12)$$

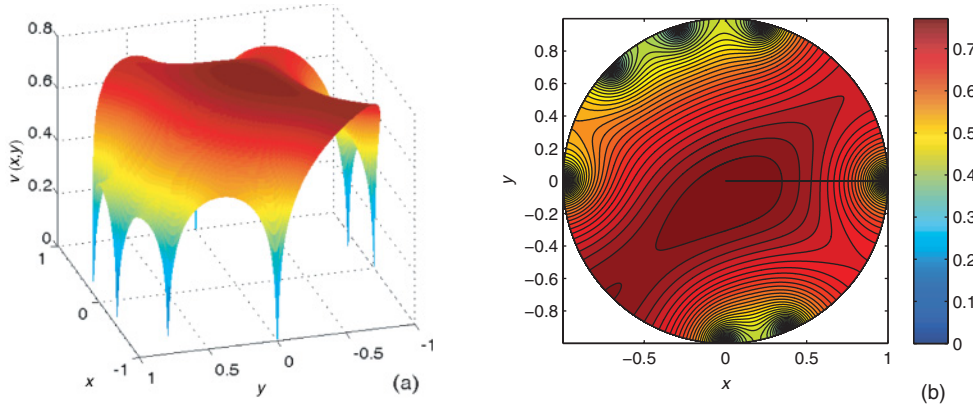


FIG. 2. (Color online) Surface (a) and contour (b) plots of the asymptotic MFPT (2.11) and (2.12) for a unit disk with $N = 7$ traps of a common length $2\varepsilon = 0.02$.

As an example, in Fig. 2, the MFPT $v(x)$ is plotted for a seven-trap configuration with a common trap length of $2\varepsilon = 0.02$.

We remark that the simple result (2.12) in fact sums the infinite logarithmic expansion for the MFPT for the special case of either exactly two arbitrarily spaced traps or N equally spaced traps on the boundary of the unit disk. This result follows since, for these special arrangements of traps, the symmetric Green's matrix \mathcal{G} has a cyclic matrix structure [12].

In the case of more than two identical traps which are not equally spaced, one can observe the difference between the two-term approximation of the average MFPT \bar{v} given by Eq. (2.12) and the full asymptotic expression (2.9). This is illustrated in Fig. 3, where these formulas are compared for a nonsymmetric and a symmetric arrangement of four traps.

The minimum of the repulsive logarithmic energy term in Eq. (2.12) is evidently attained when the traps are equally spaced on the unit circle. For such a symmetric arrangement, and assuming well-separated traps, a simple calculation yields

$$\bar{v} \sim \frac{1}{DN} \left[-\log \frac{\varepsilon N}{2} + \frac{N}{8} \right], \quad v(x) \sim \bar{v} - \frac{\pi}{DN} \sum_{j=1}^N G(x; x_j). \quad (2.13)$$

The error in this approximation is of order $O(\varepsilon)$ (cf. [14]), which is transcendentally small in comparison to any power of $-1/\log \varepsilon$.

2. The unit square

For a unit square $\Omega \equiv \{x = (x_1, x_2) | 0 \leq x_1, x_2 \leq 1\}$, the explicit form of the Neumann Green's function with an interior singularity was found in [22] by calculating a Fourier series representation of the solution of Eq. (2.3), and using summation formulas to extract both the logarithmic singularity and its regular part. Upon taking the limit as the singularity ξ approaches a noncorner point of the domain boundary, one obtains a solution of the form

$$G(x; \xi) = -\frac{1}{\pi} \log |x - \xi| + R(x; \xi), \quad (2.14)$$

where the regular part is given by a rapidly convergent infinite series of the explicit form

$$\begin{aligned} R(x; \xi) &= -\frac{1}{2\pi} \sum_{n=0}^{\infty} \log(|1 - q^n z_{+,+}| |1 - q^n z_{+,-}| |1 - q^n \zeta_{+,+}|) \\ &\quad -\frac{1}{2\pi} \sum_{n=0}^{\infty} \log(|1 - q^n \zeta_{+,-}| |1 - q^n \zeta_{-,+}| |1 - q^n \zeta_{-,-}|) \\ &\quad -\frac{1}{2\pi} \log \frac{|1 - z_{-,-}|}{r_{-,-}} - \frac{1}{2\pi} \log \frac{|1 - z_{-,+}|}{r_{-,+}} + H(x_1, \xi_1) \\ &\quad -\frac{1}{2\pi} \sum_{n=0}^{\infty} \log(|1 - q^n z_{-,-}| |1 - q^n z_{-,+}|). \end{aligned} \quad (2.15)$$

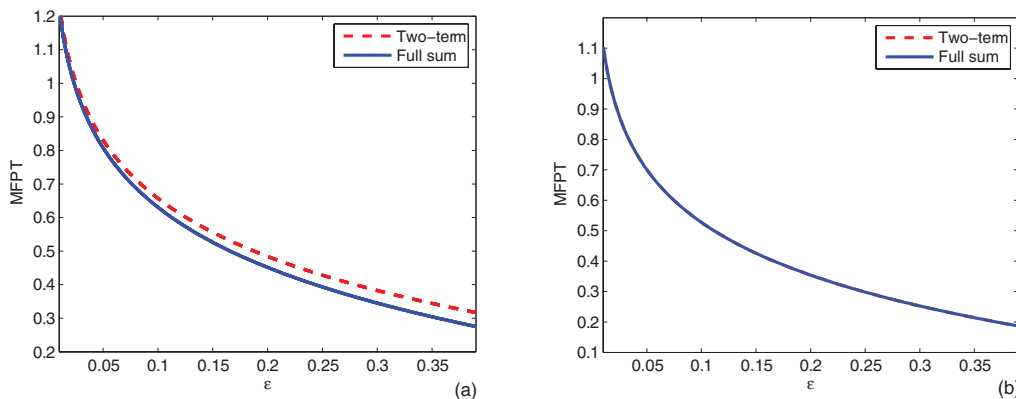


FIG. 3. (Color online) Comparison of the full asymptotic expression (2.9) and the two-term approximation (2.12) for the average MFPT \bar{v} in the case of four unevenly spaced traps of size 2ε centered at $\theta = \pi/4, \pi/2, 3\pi/4,$ and $3\pi/2$ (a), and four evenly spaced traps of size 2ε centered at $\theta = 0, \pi/2, \pi,$ and $3\pi/2$ (b).

In Eq. (2.15), $x = (x_1, x_2)$, $\xi = (\xi_1, \xi_2)$, $|z|$ denotes the modulus of a complex number z , and also

$$\begin{aligned} H(x_1, \xi_1) &= \frac{1}{12}[h(x_1 - \xi_1) + h(x_1 + \xi_1)], \\ h(\theta) &= 2 - 6|\theta| + 3\theta^2, \\ z_{\pm, \pm} &= e^{\pi r_{\pm, \pm}}, \quad \zeta_{\pm, \pm} = e^{\pi \rho_{\pm, \pm}}, \quad q = e^{-2\pi} < 1, \\ r_{+, \pm} &= -|x_1 + \xi_1| + i(x_2 \pm \xi_2), \\ r_{-, \pm} &= -|x_1 - \xi_1| + i(x_2 \pm \xi_2), \\ \rho_{+, \pm} &= |x_1 + \xi_1| - 2 + i(x_2 \pm \xi_2), \\ \rho_{-, \pm} &= |x_1 - \xi_1| - 2 + i(x_2 \pm \xi_2). \end{aligned}$$

A similar result can be given when the trap is centered at one of the corner points of the boundary of the unit square [12].

B. Three-dimensional domains: The unit sphere

Next, we consider a unit sphere centered at the origin that has N locally circular windows on its surface. The traps have radii εa_j for $j = 1, \dots, N$ and are centered at x_j for $j = 1, \dots, N$ with $|x_j| = 1$. For this case, the quantity that characterizes each trap is its electrostatic capacitance c_j , which is defined by the following local problem obtained by making a tangent-plane approximation to the sphere at x_j :

$$\begin{aligned} u_{\xi_1 \xi_1} + u_{\xi_2 \xi_2} + u_{\xi_3 \xi_3} &= 0, \quad \xi_1 \geq 0, \quad -\infty < \xi_2, \xi_3 < \infty, \\ u &= 1, \quad \text{on } \xi_1 = 0, \quad \xi_2^2 + \xi_3^2 < a_j^2; \quad u_{\xi_1} = 0, \\ &\quad \text{on } \xi_1 = 0, \quad \xi_2^2 + \xi_3^2 > a_j^2, \\ u &\sim c_j/|\xi|, \quad \text{as } |\xi| \rightarrow \infty, \end{aligned} \quad (2.16)$$

where $\xi = (\xi_1, \xi_2, \xi_3)$. For the circular trap case, this is the well-known electrified-disk problem with capacitance $c_j = 2a_j/\pi$. The capacitance is also known analytically for an elliptical-shaped window, but for a window of arbitrary shape it must be computed numerically.

For the unit sphere centered at the origin, the surface Neumann Green's function satisfying Eq. (2.3) is given explicitly by (cf. [13])

$$\begin{aligned} G_s(x; \xi) &= \frac{1}{2\pi|x - \xi|} + \frac{1}{8\pi}(|x|^2 + 1) \\ &\quad + \frac{1}{4\pi} \log \left(\frac{2}{1 - |x| \cos \gamma + |x - \xi|} \right) - \frac{7}{10\pi}, \end{aligned} \quad (2.17)$$

where γ is the angle between the vectors $x \in \Omega$ and $\xi \in \partial\Omega$, defined by $|x| \cos \gamma = x \cdot \xi$ with $|\xi| = 1$. The self-interaction term corresponding to Eq. (2.17) is simply

$$R(\xi; \xi) = -\frac{9}{20\pi}. \quad (2.18)$$

Let $\bar{c} = N^{-1}(c_1 + \dots + c_N)$ be the average capacitance, and define κ_j by

$$\kappa_j = \frac{c_j}{2} \left[2 \log 2 - \frac{3}{2} + \log a_j \right].$$

Then, for $\varepsilon \rightarrow 0$, the analysis of [13] showed that the asymptotic formula for the MFPT $v(x)$ in the outer region $|x - x_j| \gg O(\varepsilon)$, for $j = 1, \dots, N$, is given by

$$v(x) = \bar{v} - \frac{|\Omega|}{DN\bar{c}} \sum_{j=1}^N c_j G_s(x; x_j) + O(\varepsilon \log \varepsilon). \quad (2.19)$$

Correspondingly, the asymptotic average MFPT \bar{v} is given by

$$\begin{aligned} \bar{v} &= \frac{|\Omega|}{2\pi\varepsilon DN\bar{c}} \left[1 + \varepsilon \log \left(\frac{2}{\varepsilon} \right) \frac{\sum_{j=1}^N c_j^2}{2N\bar{c}} + \frac{2\pi\varepsilon}{N\bar{c}} p_c(x_1, \dots, x_N) \right. \\ &\quad \left. - \frac{\varepsilon}{N\bar{c}} \sum_{j=1}^N c_j \kappa_j + O(\varepsilon^2 \log \varepsilon) \right]. \end{aligned} \quad (2.20)$$

The $O(\varepsilon)$ term in the square bracket in Eq. (2.20) depends on the specific arrangement of traps on the unit sphere through the energylike function

$$p_c(x_1, \dots, x_N) = \mathcal{C}^T \mathcal{G}_s \mathcal{C},$$

where the capacitance vector \mathcal{C} and the Green's matrix \mathcal{G}_s are defined by $\mathcal{C} = (c_1, \dots, c_N)^T$ and

$$\begin{aligned} \mathcal{G}_s &\equiv \begin{pmatrix} R & G_{s12} & \cdots & G_{s1N} \\ G_{s21} & R & \cdots & G_{s2N} \\ \vdots & \vdots & \ddots & \vdots \\ G_{sN1} & \cdots & G_{sN,N-1} & R \end{pmatrix}, \\ R &\equiv R(x_j; x_j) = -\frac{9}{20\pi}, \quad G_{sij} \equiv G_s(x_i; x_j). \end{aligned} \quad (2.21)$$

A rigorous proof of Eqs. (2.19) and (2.20) has recently been given in [14], and the error estimate of $O(\varepsilon^2 \log \varepsilon)$ sharpened to $O(\varepsilon^2)$.

The formulas above simplify in the special case of N circular traps of a common radius $a_j = 1$, for which $c_j = 2/\pi$ for $j = 1, \dots, N$. For this case, the average MFPT reduces to

$$\begin{aligned} \bar{v} &\sim \frac{|\Omega|}{4\varepsilon DN} \left[1 + \frac{\varepsilon}{\pi} \log \left(\frac{2}{\varepsilon} \right) + \frac{\varepsilon}{\pi} \left(-\frac{9N}{5} + 2(N-2) \log 2 \right. \right. \\ &\quad \left. \left. + \frac{3}{2} + \frac{4}{N} \mathcal{H}(x_1, \dots, x_N) \right) \right], \end{aligned} \quad (2.22)$$

where the interaction energy $\mathcal{H}(x_1, \dots, x_N)$ is defined by

$$\mathcal{H}(x_1, \dots, x_N) = \sum_{i=1}^N \sum_{j=i+1}^N h(x_i; x_j), \quad (2.23)$$

and the pairwise interaction energy by

$$\begin{aligned} h(x_i; x_j) &= \frac{1}{|x_i - x_j|} - \frac{1}{2} \log |x_i - x_j| \\ &\quad - \frac{1}{2} \log(2 + |x_i - x_j|). \end{aligned} \quad (2.24)$$

The total energy (2.23) is a sum of the classical Coulombic and logarithmic discrete energy terms, and an additional interaction term between particles (traps) located on the sphere.

Now consider another special case where there are two kinds of traps, with radii given by $a_j = 1$ for $j = 1, \dots, N$ and $a_j = \alpha$ for $j = N+1, \dots, 2N$. Each element of the matrix \mathcal{G}_s

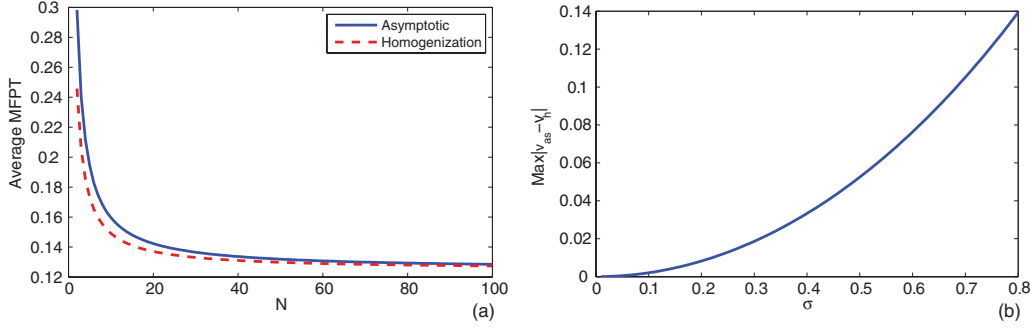


FIG. 4. (Color online) (a) Comparison of \bar{v}_{as} and \bar{v}_h as functions of N for $\sigma = 0.5$; (b) the maximal difference of \bar{v}_{as} and \bar{v}_h as functions of N for $0.01 \leq \sigma \leq 0.8$.

is still given by Eq. (2.21). The capacitance vector becomes $\mathcal{C} = (2/\pi)(1, \dots, 1, \alpha, \dots, \alpha)^T$, and the average MFPT is

$$\bar{v} \sim \frac{|\Omega|}{4\epsilon DN(1+\alpha)} \left[1 + \frac{\epsilon}{\pi} \log\left(\frac{2}{\epsilon}\right) \left(\frac{1+\alpha^2}{1+\alpha}\right) + \frac{\epsilon}{\pi} \left(S + \frac{4}{N(1+\alpha)} \tilde{\mathcal{H}}(x_1, \dots, x_N) \right) \right], \quad (2.25)$$

where the constant S is defined by

$$S = -\frac{9}{5}N(1+\alpha) + 2 \log 2 \left((N-2)(1+\alpha) + \frac{4\alpha}{1+\alpha} \right) + \frac{3}{2} \left(\frac{1+\alpha^2}{1+\alpha} \right) - \frac{\alpha^2}{1+\alpha} \log \alpha,$$

and the interaction energy $\tilde{\mathcal{H}}$ is defined by

$$\tilde{\mathcal{H}}(x_1, \dots, x_N) = \sum_{i=1}^N \sum_{j=i+1}^N h(x_i; x_j) + \alpha \sum_{i=1}^N \sum_{j=N+1}^{2N} h(x_i; x_j) + \alpha^2 \sum_{i=N+1}^{2N} \sum_{j=i+1}^{2N} h(x_i; x_j), \quad (2.26)$$

where $h(x_i; x_j)$ is given by Eq. (2.24).

In Sec. V, the interaction energies (2.23) and (2.26) are used to find optimal trap arrangements on the surface of the unit sphere that minimize the interaction energy and, correspondingly, minimize the average MFPT.

III. DILUTE TRAP FRACTION LIMIT OF HOMOGENIZATION THEORY FOR THE UNIT DISK

Homogenization theory can be used to provide a simplified approximate description of the MFPT problem (1.1) in the case of a large number of small boundary traps. Within this approach, the strongly heterogeneous boundary conditions are replaced with an effective boundary condition of a simpler form, involving parameters that may be theoretically or empirically determined.

Consider a unit disk with a large number of evenly spaced small boundary traps of equal size 2ϵ . In [20], it has been shown that, in the dilute trap fraction limit, i.e., in the limit of the number of traps $N \rightarrow +\infty$, with the total trap length fraction $\sigma = 2\epsilon N/(2\pi)$ kept constant, the mixed Dirichlet-Neumann

problem (1.1) for the MFPT $v(x)$ can be approximated by a Robin problem for $v_h(x) \simeq v(x)$ given by

$$\Delta v_h = -\frac{1}{D}, \quad r = |x| < 1; \quad \epsilon \partial_r v_h + \kappa v_h = 0, \quad r = 1, \quad (3.27)$$

where the effective transfer coefficient κ is given by

$$\kappa = -\frac{\pi\sigma}{2} \left\{ \log \left[\sin \left(\frac{\pi\sigma}{2} \right) \right] \right\}^{-1}.$$

The problem (3.27) is radially symmetric, and has the solution

$$v_h(r) = -\frac{1}{4D} \left(1 - r^2 + \frac{2\epsilon}{\kappa} \right). \quad (3.28)$$

Defining \bar{v}_h as the average of v_h , we calculate that

$$\bar{v}_h = \frac{1}{8D} + \frac{\epsilon}{2\kappa D} = \frac{1}{8D} - \frac{1}{DN} \log \left[\sin \left(\frac{\pi\sigma}{2} \right) \right]. \quad (3.29)$$

The homogenization theory prediction of the average MFPT (3.29) can be compared to the approximate solution obtained from the asymptotic theory considered in the current paper. For N equal evenly spaced traps of size 2ϵ , it is given by Eq. (2.13), which may be written as

$$\bar{v}_{\text{as}} \sim \frac{1}{8D} - \frac{1}{DN} \log \left(\frac{\pi\sigma}{2} \right), \quad (3.30)$$

and is evidently related to the homogenization result (3.29) through the Taylor series expansion of the sine function when σ is small. Some comparative results for the average MFPT formulas \bar{v}_h (3.29) and \bar{v}_{as} (3.30) are given in Fig. 4.

IV. COMPARISON OF THE ASYMPTOTIC MFPT WITH FULL NUMERICAL RESULTS

In terms of computational complexity and computational time required for their evaluation, the asymptotic formulas for the MFPT and the average MFPT presented in Sec. II are fundamentally superior to those obtained from other approximation techniques, such as full numerical solutions of the PDE problem (1.1) or Brownian random walk simulations.

The primary limitation of the asymptotic formulas is set by their domain of validity. More specifically, the general MFPT approximation (2.5) was derived in the limit of small trap size under the assumption of well-separated small traps, i.e., when the centers of the traps are separated by $O(1)$ distances.

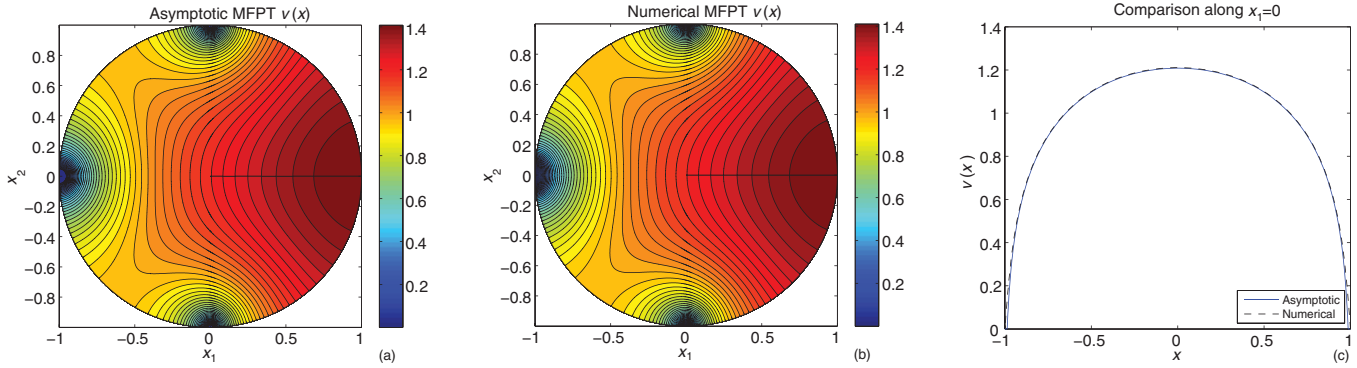


FIG. 5. (Color online) Comparison of asymptotic (a) and numerical (b) predictions for the MFPT $v(x)$ for a three-trap configuration in the unit disk, with two traps of length ε (centered at $\theta = \pi/2$ and $\theta = 3\pi/2$), and one trap of length 3ε (centered at $\theta = \pi$). Here $\varepsilon = 0.06$. Comparison of asymptotic and numeric MFPT along the cross section $x_1 = 0$ (c).

Additionally, since the asymptotic MFPT formulas are singular at the trap locations, it is important to have an understanding at which minimal distances from traps the asymptotic formulas are still sufficiently accurate.

In order to test the applicability limits of the asymptotic formulas of Sec. II, with respect to both trap size and trap separation effects, we compare results from the asymptotic theory with corresponding full numerical results computed from a direct finite-difference numerical solution of the boundary value problem (BVP) (1.1). The comparisons are made for several trap configurations for both the two- and three-dimensional cases. The Dirichlet-Neumann BVP (1.1) for the Poisson equation was solved using a finite-difference method employing variable steps in all space directions, and mesh refinement in order to resolve small traps.

A. Trap size effects

The error terms in the asymptotic expansions for the MFPT $v(x)$ and its average \bar{v} for both the two-dimensional and the three-dimensional have the order $O(\varepsilon)$ when $\varepsilon \ll 1$ (cf. [14]). This error estimate does not provide any information regarding the size of the coefficient of ε , and so does not indicate how well the asymptotic formulas will predict the true results when ε is not small. The goal below is to compare the results of Sec. II for the MFPT $v(x)$ and the average MFPT \bar{v} with results

obtained from the full numerical solution of the problem (1.1) in order to quantitatively assess the error, and to provide a guide some benchmark on how the asymptotic results fare at finite values of ε .

1. The unit disk

For the unit disk, the following four trap configurations were studied: a single trap (arc) of arclength ε ; two oppositely placed traps each of arclength ε ; seven equally spaced traps each of arclength ε ; and a three-trap configuration: two traps of length ε centered at $\theta = \pi/2$ and $3\pi/2$, and one larger trap of length 3ε located at $\theta = \pi$.

For the first three arrangements of traps, the result (2.12), in which ε is replaced by $\varepsilon/2$, determines $v(x)$ and \bar{v} with an error that is smaller than any power of $-1/\log \varepsilon$. In order to obtain the same level of accuracy for the fourth configuration above, one must first solve the linear system (2.8) to determine the vector A , and then calculate $v(x)$ and \bar{v} from Eqs. (2.5), (2.9), and (2.11).

For each of these four trap configurations, it was found that the asymptotic and numerical results for the average MFPT \bar{v} are within 1% agreement when the length of the traps is of the order of one. A sample comparative contour plot of $v(x)$ for the three-trap configuration (Fig. 5) shows a close agreement between the asymptotic and numerical results for the MFPT

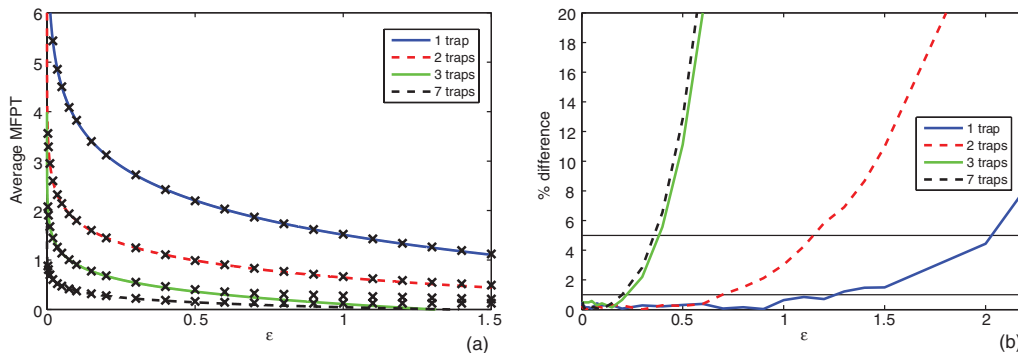


FIG. 6. (Color online) (a) Dependence of the average MFPT \bar{v} on the trap length ε for one-, two-, three-, and seven-trap configurations in a unit disk. The curves correspond to the asymptotic formulas and the crosses to numerical results. (b) Percent difference between asymptotic and numerical results vs ε .

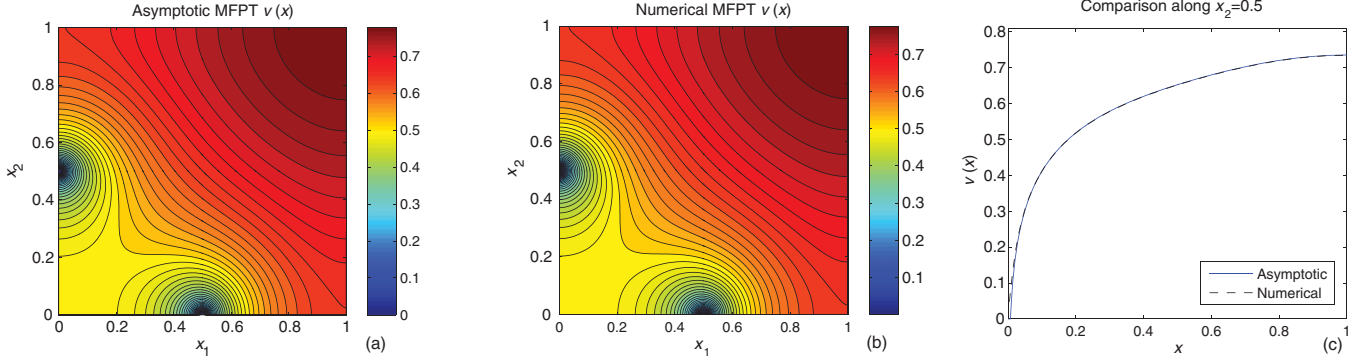


FIG. 7. (Color online) Comparison of the asymptotic (a) and numerical (b) results for the MFPT $v(x)$ for two traps of a common length $\varepsilon = 0.03$ for the unit square. Comparison of asymptotic and numerical results along the cross section $x_2 = 0.5$ (c).

everywhere in the domain except for a very small region near the traps.

The results for the disk are summarized in Fig. 6, where the average MFPT \bar{v} is plotted as a function of ε for the one-, two-, three-, and seven-trap configurations. In particular, for one trap, the results are within 5% agreement for a trap length $\varepsilon \lesssim 2$, which is roughly 1/3 of the length of the domain boundary. Similarly, for seven equally spaced traps, the results are within 5% agreement for a trap length $\varepsilon \lesssim 0.35$, which is roughly 40% of the length of the domain boundary.

2. The unit square

For the unit square, the following four trap configurations were considered: a single trap of length ε centered at $(x_1, x_2) = (0, 0.5)$; two traps of lengths ε centered at $(x_1, x_2) = (0, 0.5)$ and $(0.5, 0)$; and four traps of lengths ε located at each of the centers of the four sides of the square.

The asymptotic MFPT $v(x)$ and the asymptotic average MFPT \bar{v} were computed from Eqs. (2.5), (2.14), and (2.15). A comparative plot of the MFPT $v(x)$ for the case of two traps of a common length $\varepsilon = 0.03$ is given in Fig. 7, while the comparisons of the average MFPT \bar{v} for all three trap configurations are summarized in Fig. 8. Compared to the situation for the unit disk, the asymptotic results for v and \bar{v} for

the square domain reliably predict the full numerical values for a slightly smaller range of ε . For example, for one trap, the 1% agreement between the asymptotic and the numerical solution is only observed for $\varepsilon \lesssim 0.2$ ($\varepsilon \lesssim 0.4$ for 5% agreement). For the four-trap case, we have 1% agreement when $\varepsilon \lesssim 0.1$ (10% trap surface area fraction), and 5% agreement when $\varepsilon \lesssim 0.25$ (25% trap surface area fraction). These results show that one can still reliably use the asymptotic theory at rather large values of the small parameter ε . The slightly smaller range of validity in ε in comparison to the case of the unit disk can probably be attributed to the effects of the nonsmooth domain boundary of the square.

3. The unit sphere

For the unit sphere, we consider the simplest configurations of one, two, and three, equally spaced circular traps of radius ε centered on the equator of the unit sphere. A sample comparative contour plot of the MFPT $v(x)$ in the equatorial cross section of the sphere for a single trap of radius $\varepsilon = 0.2$, $a = 1$, is shown in Fig. 9. As seen from Fig. 10, the 1% agreement between the asymptotic and the numerical results for the average MFPT \bar{v} for a single trap is attained for trap radii with $\varepsilon \lesssim 0.8$, which corresponds to a 16% trap surface area fraction.

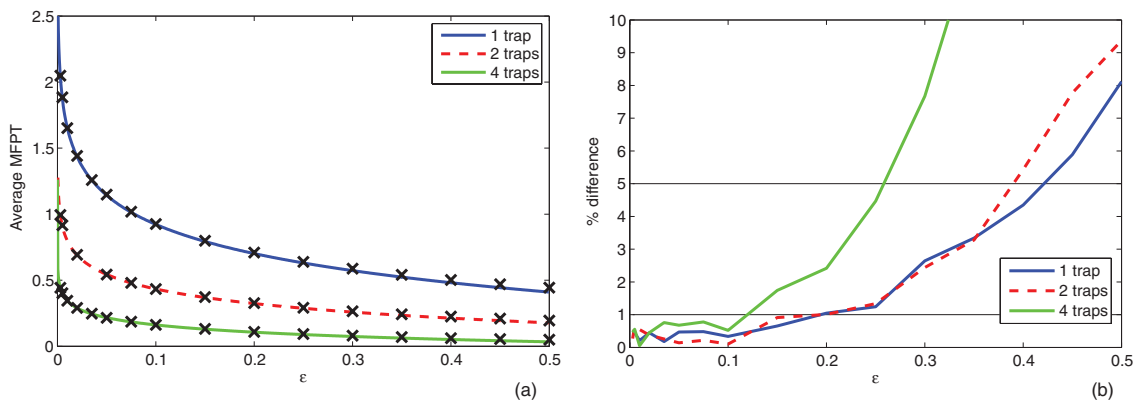


FIG. 8. (Color online) (a) Dependence of the average MFPT \bar{v} on the trap length ε for one-, two-, and four-trap configurations in a unit square. The curves correspond to the asymptotic results and the crosses to the full numerical results. (b) Percent difference between asymptotic and numerical results.

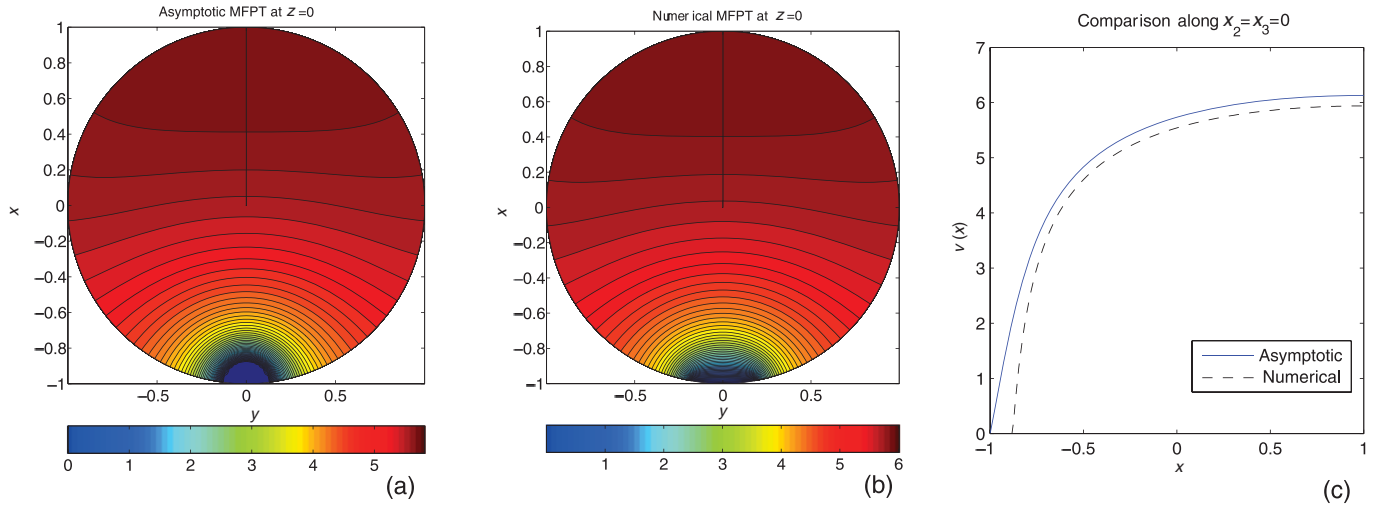


FIG. 9. (Color online) Comparison of asymptotic (a) and numerical (b) results for the MFPT $v(x)$ for one trap of radius $\epsilon = 0.2$, on the boundary of the unit sphere. Comparison of asymptotic and numerical results along the line $x_2 = x_3 = 0$ (c).

B. Trap separation effects

The results (2.9) and (2.20) for the average MFPT in a general 2D and a spherical 3D domain, respectively, are valid under the assumption of “well-separated” boundary traps. To study how the asymptotic results perform when the traps are not necessarily so well-separated, we compare the asymptotic and full numerical results for the whole range of two-trap configurations, ranging from two touching traps to the maximal possible separation distance in each given configuration.

The following comparisons suggest that, for the domains considered below, the asymptotic formulas for the average MFPT are still rather reliable, in the sense of being within 1% of the full numerical result, even for small separation distances of order $O(\epsilon)$.

1. The unit square

For the unit square, two configurations were considered. In the first configuration, two identical traps of length ϵ were located on adjacent sides, centered at a point at a distance L from the corner ($\epsilon/2 \leq L \leq 1 - \epsilon/2$; see Fig. 7). In the

second configuration, two identical traps were symmetrically located on one side of the square, at a distance L between their centers ($\epsilon \leq L \leq 1 - \epsilon$).

For traps of length $\epsilon = 0.05$, a plot of the numerical and asymptotic average MFPT and their relative difference is shown in Fig. 11. For traps located on one side of the square, the agreement between the asymptotic and numerical results is within 1% for all values of L . For traps located on adjacent sides of the square, the asymptotic result overshoots by approximately 6% when the traps are touching at the origin, but is within approximately 2% of the full numerical results when each trap is centered at a distance 0.05 from the origin.

2. The unit sphere and the unit disk

As shown in Fig. 12, a very good agreement between the asymptotic and numerical results for the average MFPT is also observed for the case of two arbitrarily spaced traps on the surface of the unit disk or unit sphere. For the unit disk, traps of arclength $\epsilon = 0.05$ were chosen. For the unit sphere, we chose circular traps of radius $\epsilon = 0.2$ located on the equator. For all separation distances, ranging from touching traps to traps on opposite sides of a diameter, the discrepancy between

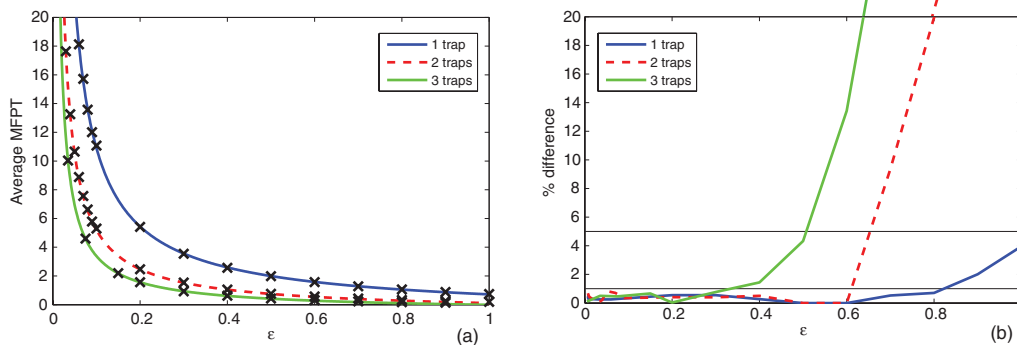


FIG. 10. (Color online) (a) Dependence of the average MFPT \bar{v} on the common trap radius ϵ for one, two, and three traps that are equally spaced on the equator of the unit sphere. The curves correspond to the asymptotic results and the crosses to full numerical results. (b) Percent difference between asymptotic and numerical results.

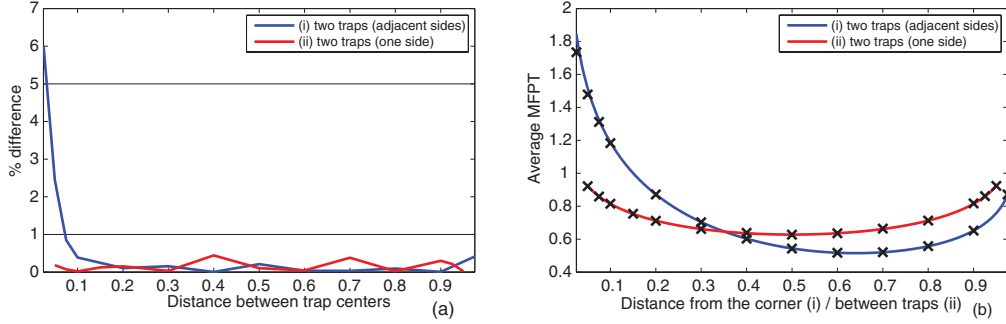


FIG. 11. (Color online) (a) Effect of trap separation in the unit square: comparison of the asymptotic and numerical results for the average MFPT \bar{v} for two traps of sizes $\varepsilon = 0.05$. (b) The percent difference. (i) Average MFPT for two traps located on adjacent sides, as a function of the distance from the corner. (ii) Average MFPT for two traps located symmetrically on one side, as a function of the distance between traps.

the asymptotic and numerical results is well within 1% for both domains.

C. Asymptotic approximation near traps

The asymptotic formulas for MFPT $v(x)$ given in Sec. II are valid when the MFPT is measured sufficiently far from the trap. It is clear that, close to traps, the situation must be different, since the Green's functions in formula (2.5) are always singular: $|v(x)| \rightarrow +\infty$ at $x \rightarrow x_j$. In particular, $v(x) \sim O(\log|x - x_j|)$ in two dimensions, and $v(x) \sim O(|x - x_j|^{-1})$ in three dimensions. In contrast, for the solutions of the problem (1.1), we must have $v(x) \rightarrow 0$ as $x \rightarrow x_j$.

We now consider an example that illustrates the quality of the asymptotic approximation close to a trap in a unit disk. Let the disk have a single boundary trap of the size 2ε , centered at $x_1 = (-1, 0)$. The difference of the numerical and the asymptotic MFPT (2.5) is shown in Fig. 13 for a large trap of size $2\varepsilon = 0.4$. Similar but smaller scale error behavior is observed for smaller values of ε , as seen, for instance, in Fig. 5.

As a measure of the quality of the asymptotic approximation near a trap, define the largest distance from the trap center to a point in the disk for which the relative difference between the numerical and asymptotic MFPT is $100a\%$:

$$X_a(\varepsilon) = \max_D \{|x - x_1| : x \in \Omega, v_{as}(x) < (1 - a)v_{num}(x)\},$$

$$\lim_{\varepsilon \rightarrow 0} X_a(\varepsilon) = 0.$$

As seen in Fig. 14, the dependence of X_a on ε is close to linear, for a wide range of ε . $X_a(\varepsilon) \simeq k(a)\varepsilon$. In particular, $k(0.02) \simeq 2.6584$, $k(0.05) \simeq 1.9875$, $k(0.1) \simeq 1.6265$, $k(0.15) \simeq 1.4622$, and $k(0.2) \simeq 1.3668$, which is consistent with the natural expectation that $\lim_{a \rightarrow 0} k(a) = +\infty$ and $\lim_{a \rightarrow 1} k(a) = 0$.

V. OPTIMAL LOCATION OF TRAPS ON THE UNIT SPHERE

We now determine the optimal arrangements of N traps on the boundary of a given domain Ω that minimize the average MFPT \bar{v} . In [12,13], it was shown that such optimal trap arrangements also maximize the principal eigenvalue of the Laplacian in the corresponding domain with traps, thus maximizing the diffusion rate from a domain with small holes on an otherwise reflecting boundary. Here the attention is restricted to the sphere, which is a fundamental domain both from the point of view of applications and the complexity of numerical optimization. Indeed, boundary traps on the surface of two-dimensional domains correspond physically to slitlike holes extended in the invariant direction on the surface of three-dimensional cylinders. Location optimization for such traps can involve permutations, but is otherwise much simpler than that for a sphere.

Consider N traps located on a unit sphere. In order to optimize the average MFPT \bar{v} in Eq. (2.20), one has to find coordinates of N repelling particles on the sphere, which correspond to the global minimum of the interaction

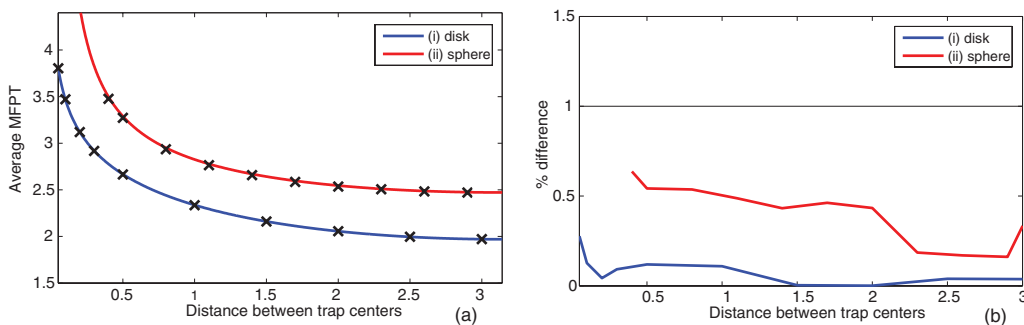


FIG. 12. (Color online) (a) Effect of trap separation in the unit disk (i) and the unit sphere (ii). Comparison of asymptotic and numerical results for the MFPT \bar{v} . Unit disk: two traps of arclength $\varepsilon = 0.05$. Unit sphere: two circular traps of radius $\varepsilon = 0.2$ located on the equator. (b) Percent difference between the asymptotic and numerical results.

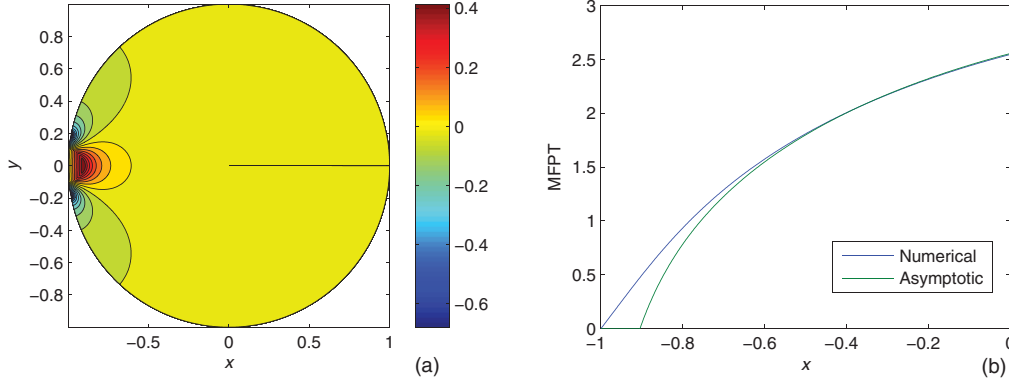


FIG. 13. (Color online) Comparison of asymptotic and numerical results for the MFPT $v(x)$, for a unit disk with one trap of arclength $2\varepsilon = 0.4$. (a) Plot of $v_{\text{num}}(x) - v_{\text{as}}(x)$ in the disk. (b) Comparison near the trap, along the radius $x \leq 0, y = 0$.

term $p_c(x_1, \dots, x_N)$ in Eq. (2.20). One thus has a global optimization problem for a function of $2N$ variables (e.g., spherical angles).

Many global optimization techniques have recently been developed, including methods for nonsmooth optimization, optimization in bounded and unbounded domains, and optimization subject to constraints. For low-dimensional problems, exact methods are available, whereas for higher-dimensional problems one is usually restricted to using partly heuristic numerical optimization algorithms. For a review of continuous global optimization algorithms and software, see [23,24].

For the computations below, the dynamical systems-based optimization method (DSO), and the extended cutting angle method (ECAM) from the open software library GANSO [25], were used. These algorithms proved to be stable and sufficiently fast for not-very-large numbers of traps ($N \lesssim 25$).

A. N identical traps

For N traps of a common radius ε on the unit sphere, it is convenient to use spherical coordinates $x_j = (1, \theta_j, \phi_j)$, for $j = 1, \dots, N$, where θ_j is the azimuthal angle and ϕ_j is the polar angle. To minimize the average MFPT \bar{v} , one has to find a global minimum of the interaction energy $\mathcal{H}(x_1, \dots, x_N)$ of Eq. (2.23) in a hypercube $0 \leq \theta_j \leq \pi, 0 \leq \phi_j < 2\pi$ in $2N$

dimensions. We remark that by fixing the position of the first trap to be at the north pole $(\theta_1, \phi_1) = (0, 0)$ and by setting $\phi_2 = 0$, the dimension of the problem is reduced to $2N - 3$.

Coordinates for optimal spherical arrangements for $3 \leq N \leq 20$ and interaction energy values for $3 \leq N \leq 65$ have been numerically computed in [13] by using both the DSO and ECAM methods. For $N = 2, 3$, traps are located on an equator; for $N = 4$, they are in the vertices of a regular tetrahedron; for $N = 5, 6, 7$, two traps occupy poles and the other $N - 2$ lie on the equator. The majority of configurations of $N > 7$ traps do not exhibit an obvious symmetry. Sample minimal energy trap configurations are shown in Fig. 15 for $N = 4, 7$, and 16 traps.

B. Optimal locations of a pattern with two kinds of traps

Now consider a $2N$ -trap configuration, with N traps having radius ε and the other N traps having radius $\alpha\varepsilon, \alpha > 1$. The asymptotic average MFPT for such a configuration is given by Eq. (2.25). This formula depends on the trap locations through the interaction energy $\tilde{\mathcal{H}}$ as given in Eq. (2.26).

When α is large, the energy $\tilde{\mathcal{H}}$ depends significantly on the locations of the large traps, and much more weakly on the locations of the small traps. This is because the “repelling force” between any two traps is proportional to their radii. This yields a harder global optimization problem, with multiple local minima that have very close values of the

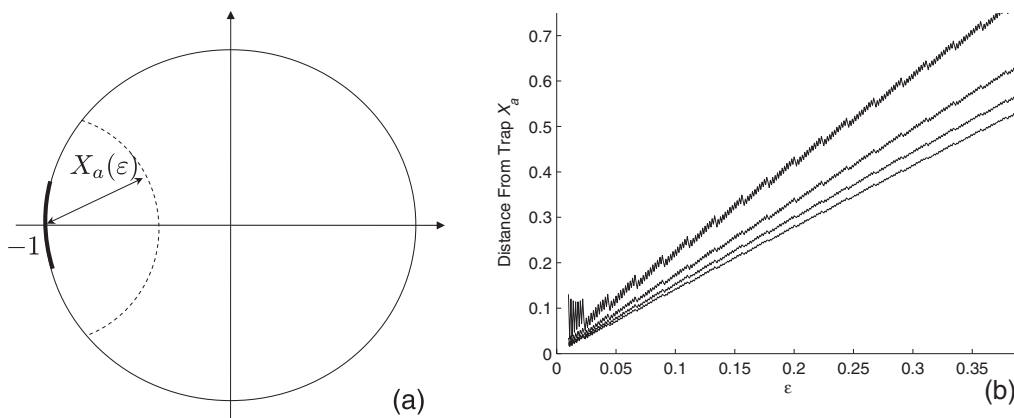


FIG. 14. (a) Relative error measure $X_a(\varepsilon)$. (b) Plots of $X_a(\varepsilon)$ for $a = 0.05, 0.1, 0.15$, and 0.2 (top to bottom). (Numerical computations were performed for the step $\delta\varepsilon = 0.001$ in ε . Observed oscillations are a numerical phenomenon, which vanishes as $\delta\varepsilon \rightarrow 0$.)

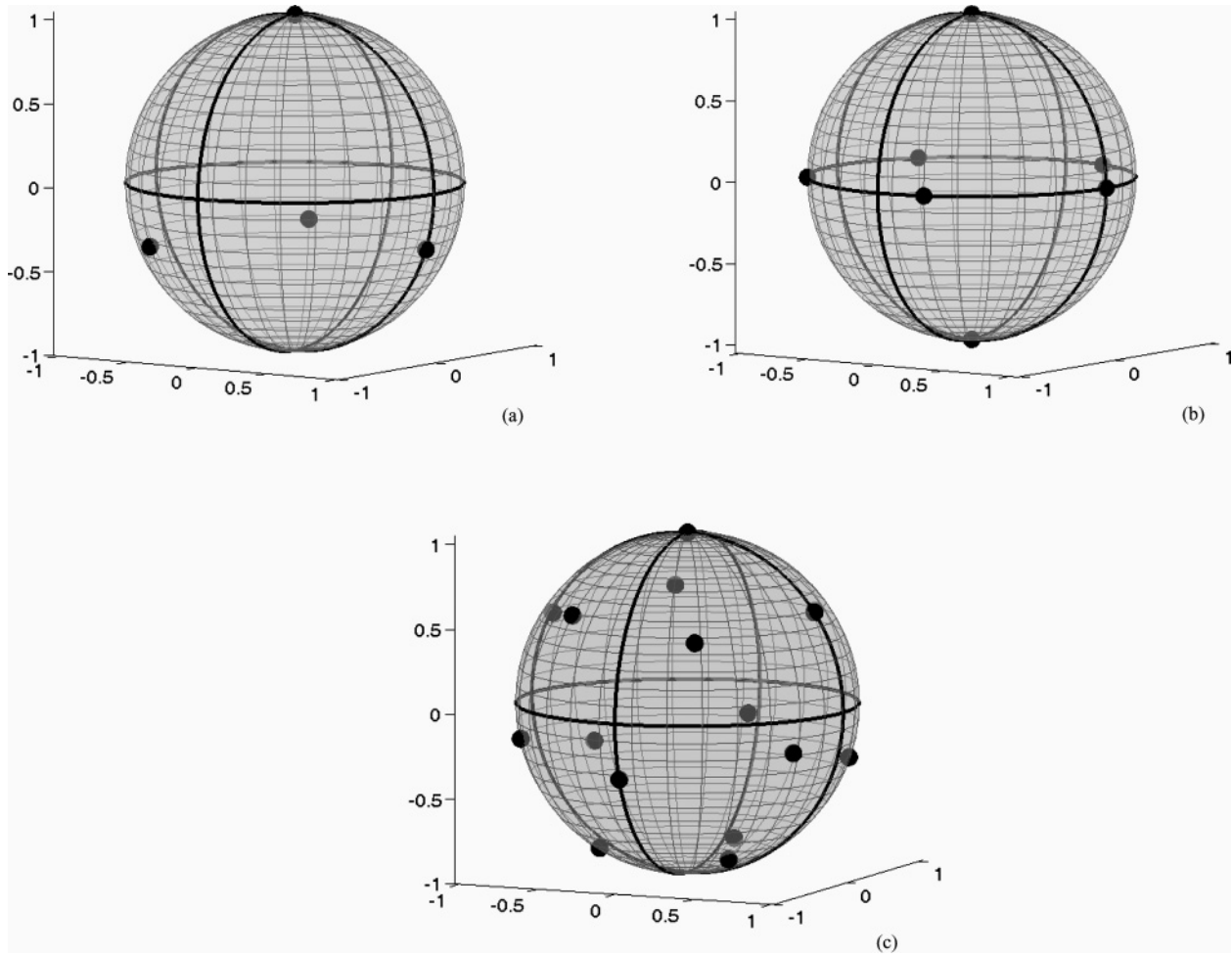


FIG. 15. Minimal energy spherical trap configurations for (a) $N = 4$, (b) $N = 7$, and (c) $N = 16$ identical traps.

energy, yet rather different locations of the small traps. Sample configurations for $\alpha = 10$ are given in Figs. 16, 17, and 18. The global minimum values were the same for both ECAM and DSO methods.

In particular, for $2N = 4$, the resulting configuration is a distorted tetrahedron, with two large traps tending to occupy

the poles as α increases [see Fig. 16(a)]. For $2N = 6$, the large traps are close to the vertices of an equilateral triangle on the equator [see Fig. 16(b)]. For $2N = 8$, the global minimum is given by a symmetric configuration with $\tilde{\mathcal{H}} = -163.615\,03$. However, several local minima close to the global minimum were found using the ECAM algorithm, for example, with

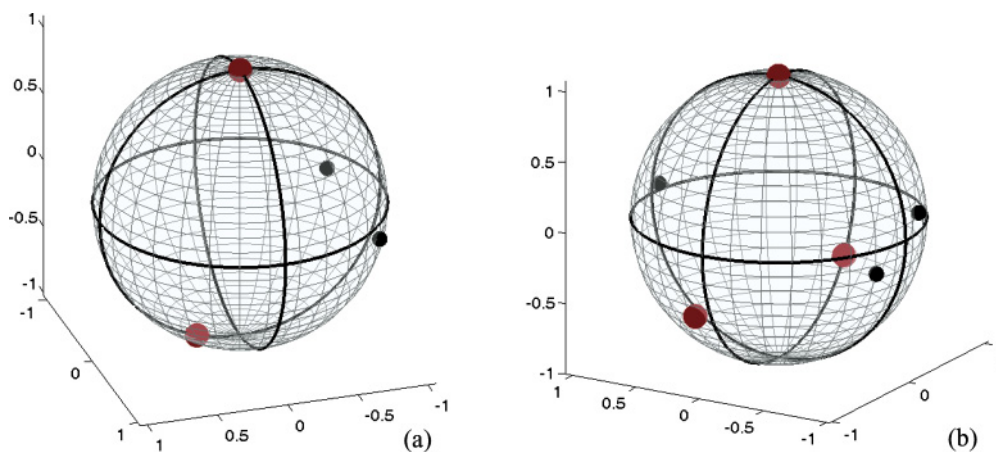


FIG. 16. (Color online) Minimal energy spherical trap configurations for $2N$ traps of two kinds: (a) $2N = 4$; (b) $2N = 6$. The radius ratio of the traps is $\alpha = 10$. Larger traps are shown in red and smaller in black.

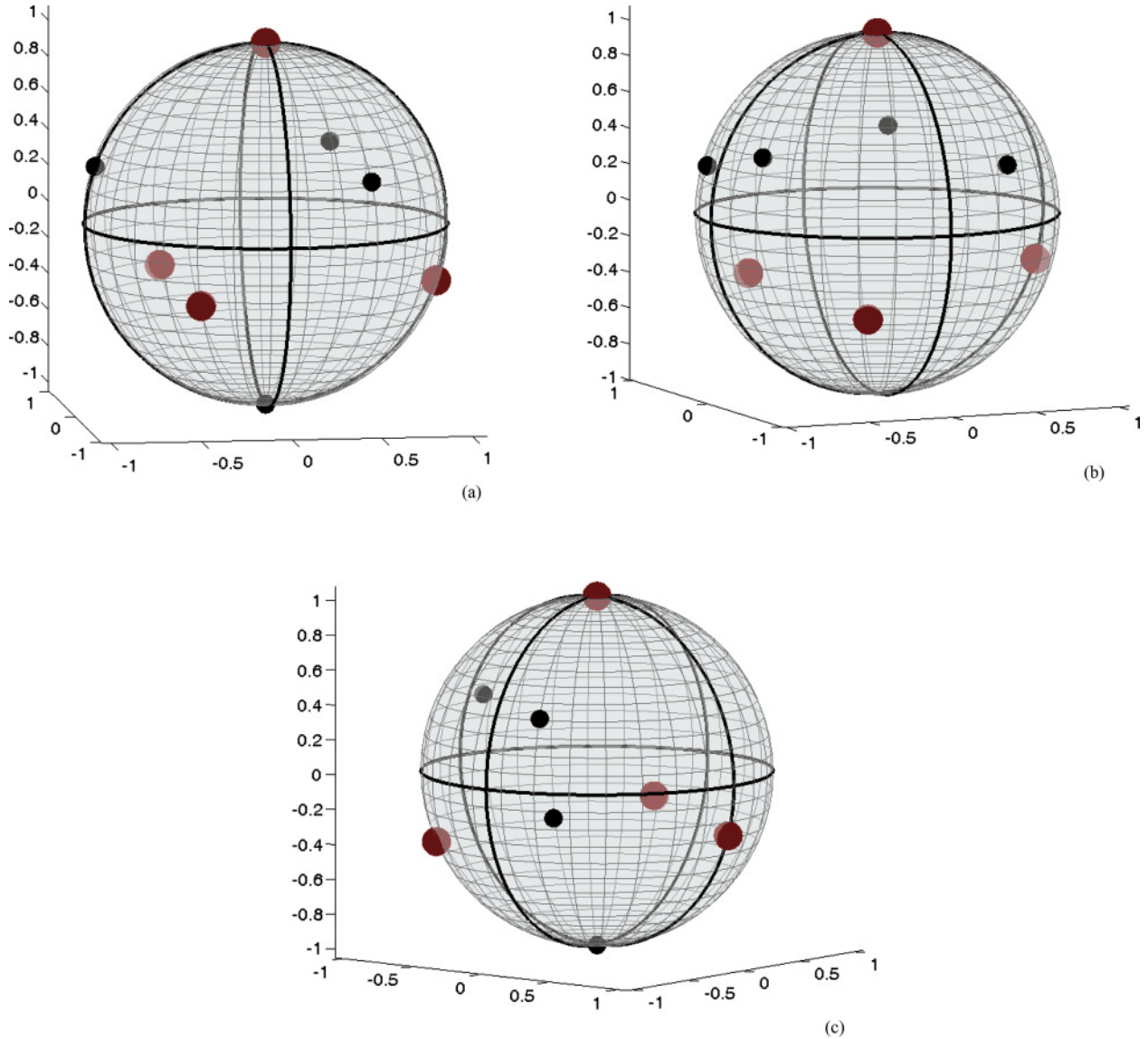


FIG. 17. (Color online) Spherical trap configurations for $2N = 8$ traps of two kinds with radius ratio $\alpha = 10$. The larger traps are shown in red and the smaller traps in black. (a) The configuration corresponding to the global minimum of the average MFPT \bar{v} . (b), (c) Configurations corresponding to nearby local minima of \bar{v} with $\tilde{\mathcal{H}} = (-162.502\ 34, -162.464\ 60)$.

energies $\tilde{\mathcal{H}} = (-162.502\ 34, -162.464\ 60)$. These local minima correspond to nonsymmetric arrangements (Fig. 17).

For $2N = 10$, the global minimum is given by $\tilde{\mathcal{H}} = -198.807\ 59$. The ECAM optimization method also gives two nearby local minima with $\tilde{\mathcal{H}} = (-198.369\ 39, -197.760\ 83)$. In each of these three configurations, the five large traps are found to be close to the simple optimal configuration of five identical traps on the sphere, where two traps are at the poles and the remaining traps occupy the three vertices of an equilateral triangle on the equator (see Fig. 18).

C. Fragmentation effects: The case of $N \gg 1$ traps

In order to study fragmentation effects, we consider N identical traps of radius ε . We denote the percentage surface area fraction of traps by $100f$, where $f \equiv N\pi\varepsilon^2/4\pi = N\varepsilon^2/4$. Plots of $\bar{v}(N)$ for several fixed values of f are given in Fig. 19, using the numerically computed values of the

interaction energy \mathcal{H} for optimal spherical trap arrangements ($N = 3, \dots, 65$). All curves are decreasing functions. This confirms the expectation that in order to minimize \bar{v} using traps of a fixed trap surface area fraction it is preferable to have many smaller traps equidistributed over the surface of the sphere rather than have a small number of larger traps that cover the sphere only sparsely.

An approximate scaling law for the interaction energy $\mathcal{H}(x_1, \dots, x_N)$ of Eq. (2.23), for N identical optimally distributed traps on a unit sphere ($N \gg 1$), was derived in [13], and is given by

$$\mathcal{H} \approx \mathcal{F}(N) = \frac{N^2}{2} (1 - \log 2) + b_1 N^{3/2} + b_2 N \log N + b_3 N + b_4 N^{1/2} + b_5 \log N + b_6, \tag{5.31}$$

$$b_1 \approx -0.5668, \quad b_2 \approx 0.0628, \quad b_3 \approx -0.8420, \\ b_4 \approx 3.8894, \quad b_5 \approx -1.3512, \quad b_6 \approx -2.4523. \tag{5.32}$$

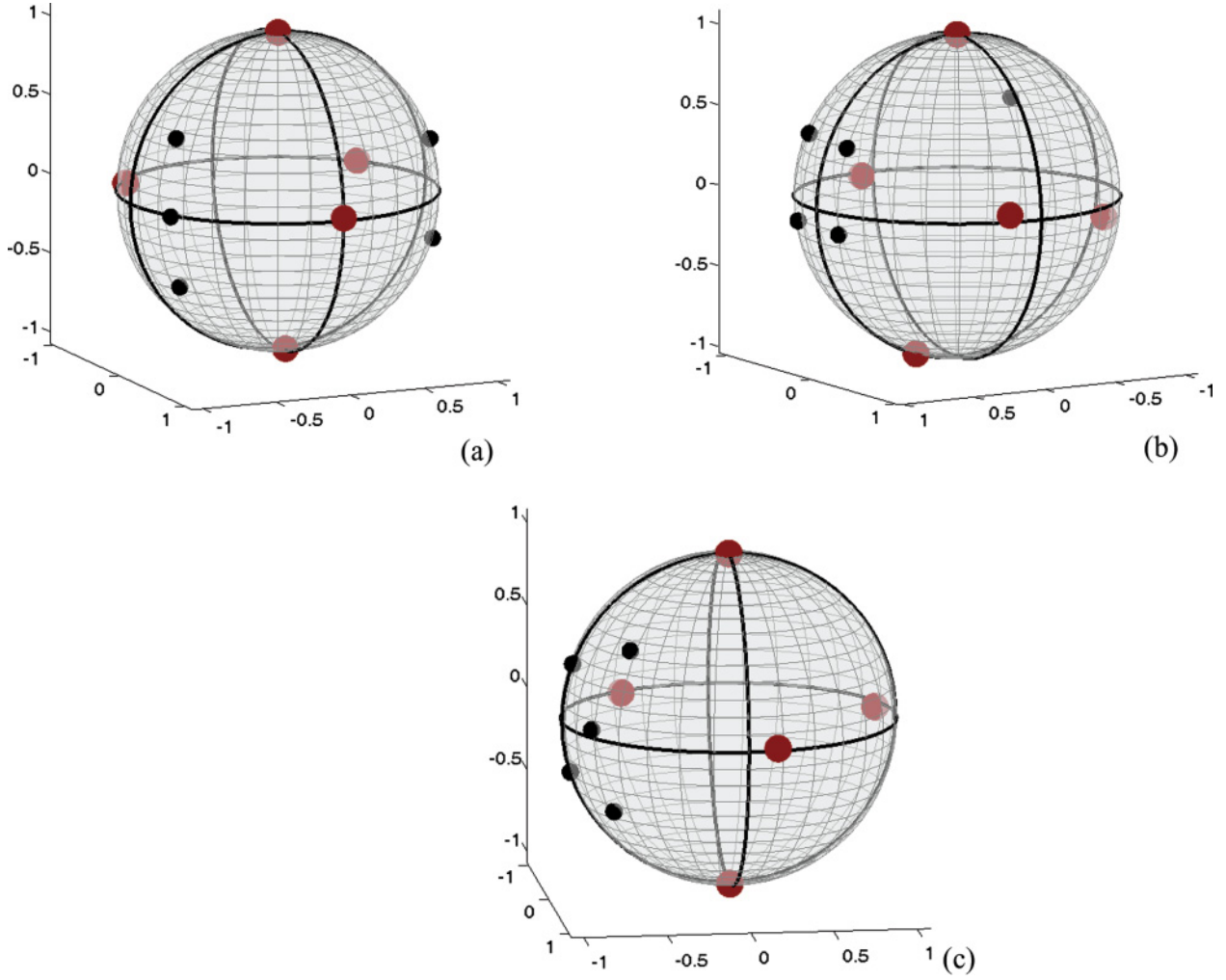


FIG. 18. (Color online) Spherical trap configurations for $2N = 10$ traps of two kinds with radius ratio $\alpha = 10$. The larger traps are shown in red and the smaller traps in black. (a) The configuration corresponding to the global minimum of the average MFPT \bar{v} . (b), (c) Configurations corresponding to nearby local minima of \bar{v} with $\mathcal{H} = (-198.369\ 39, -197.760\ 83)$.

By using Eq. (5.31) in the expression for the average MFPT \bar{v} as given in Eq. (2.22), one obtains in terms of the trap surface

area fraction f that

$$\bar{v} \sim \frac{|\Omega|}{8D\sqrt{fN}} \left[1 - \frac{\sqrt{f/N}}{\pi} \log\left(\frac{4f}{N}\right) + \frac{2\sqrt{fN}}{\pi} \left(\frac{1}{5} + \frac{4b_1}{\sqrt{N}} \right) \right]. \quad (5.33)$$

Here it is required that the third term in Eq. (5.33) is asymptotically smaller than the second term. Thus the approximation (5.33) holds for $N \gg 1$ when the trap area fraction satisfies $f \ll O(\varepsilon)$.

VI. DISCUSSION

The MFPT $v(x)$ required for a Brownian particle starting at an arbitrary location x to leave a two-dimensional or a three-dimensional domain Ω with boundary traps satisfies a boundary value problem (1.1) for the linear Poisson equation with mixed Dirichlet-Neumann boundary conditions. Asymptotic results the MFPT $v(x)$ for a 2D domain and for the unit sphere. These asymptotic formulas have been derived under the assumption of well-separated asymptotically small traps [trap

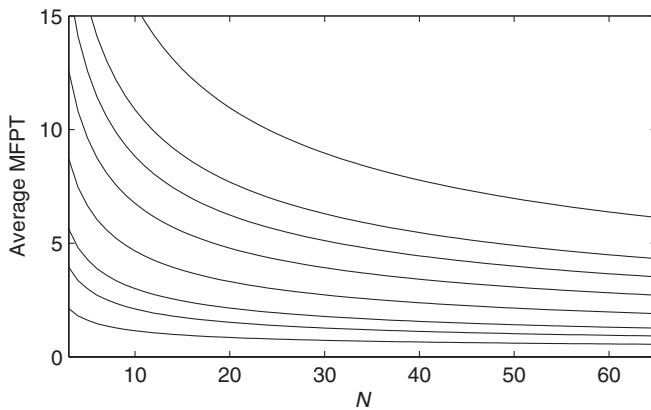


FIG. 19. Trap fragmentation effects. The average spherical MFPT \bar{v} (2.22) vs N (number of traps) for a fixed trap surface area percentage. Curves for $f = 0.1\%, 0.2\%, 0.3\%, 0.5\%, 1\%, 2.2\%, 4\%$, and 10% (top to bottom).

size $\sim \varepsilon \ll \text{diam}(\Omega)$. By computing full numerical solutions of the PDE (1.1), it was shown for certain two-dimensional domains and for the unit sphere that the asymptotic theory of [12,13] provide very reliable approximations to the average MFPT for a rather wide range of trap sizes, not simply those of very small measure. In particular, for the case of one trap of size ε , it was shown that the asymptotic and numerical values of the average MFPT \bar{v} agree within 1% for the unit disk when $\varepsilon \lesssim 1.25$, for the unit square when $\varepsilon \lesssim 0.2$, and for the unit sphere when $\varepsilon \lesssim 0.8$. This close agreement between asymptotic and numerical results at finite, but not necessarily asymptotically small, values of the trap size ε illustrates one of the often key benefits of developing a theory based on asymptotic analysis.

With regard to the effect of trap separation, the validity limits of the asymptotic formulas were also tested using comparisons with full numerical solution for the case of two identical traps on the boundary of the unit disk, the unit square, and the unit sphere. It was shown that, for all configurations, the asymptotic and numerical values of \bar{v} remain within 1% agreement for both large and small trap separations, even to the point when the traps touch.

Due to its essentially singular form, the quality of the asymptotic MFPT approximation deteriorates when domain points close to the traps are chosen. However, as shown in Sec. IV C for a unit disk, this error can be controlled. In particular, the distance from the trap where any given relative error occurs decreases as $\varepsilon \rightarrow 0$. The same can be shown for the rectangular and the spherical domain.

The asymptotic results for the MFPT for the unit sphere involve a higher-order term that depends on the global configuration of the traps. This term, referred to as the “interaction energy,” involves a sum of two classical discrete energy functions: the logarithmic energy and the Coulomb energy, together with an additional logarithmic term. The optimal point of this interaction energy corresponds to the minimum value of the average MFPT \bar{v} . This interaction energy was optimized for N equal traps, and for a pattern of $2N$ traps consisting of N small traps and N much larger traps.

The computed optimal spherical trap configurations for $3 \leq N \leq 65$ equal traps were used in the formula for the average MFPT \bar{v} to study trap fragmentation effects. Results confirm that for a fixed surface area fraction of traps f , within the computed range of N , faster escape is achieved for the case where N small traps are equidistributed over the surface of the sphere rather than placing a few large traps on the sphere.

There are two directions that warrant further study. First, the asymptotic theory relies on detailed knowledge of the Neumann Green’s function and its regular part. For an arbitrary 2D domain, it would be worthwhile to develop a hybrid asymptotic-numerical method for the calculation of the average MFPT that combines the asymptotic theory with fast-multipole methods, such as in [26] to calculate the Neumann Green’s function. For an arbitrary 3D domain with smooth boundary, it is relatively straightforward to derive a three-term asymptotic for the average MFPT similar to that for the sphere given in Eq. (2.20). For the case of one trap, this has been done recently in [14]. However, to evaluate the coefficients in this formula, one would have to determine numerically the Neumann Green’s function and its regular part for an arbitrary 3D domain with a Dirac source term on the boundary. The development of reliable numerical methods to compute this Green’s function is an open problem.

A second open problem is to further study the relationship between the asymptotic theory in the limit of a large number of traps and results that can be obtained from the dilute trap fraction limit of homogenization theory. In particular, for the unit sphere, can one systematically derive, by using the large N limit of our asymptotic theory with localized traps, a simple mixed Robin type boundary condition $\partial_n v + \kappa v = 0$, for some computable constant κ , which yields the same average MFPT? For a unit disk, this relation is discussed in Sec. III. For the unit sphere, work in this direction is in progress.

ACKNOWLEDGMENTS

The authors are grateful to NSERC for research support through Discovery Grants (A.C. and M.J.W.) and a USRA fellowship (A.R.).

-
- [1] O. Bénichou and R. Voituriez, *Phys. Rev. Lett.* **100**, 168105 (2008).
 - [2] Z. Schuss, A. Singer, and D. Holcman, *Proc. Natl. Acad. Sci. USA* **104**, 16098 (2007).
 - [3] D. Holcman and Z. Schuss, *J. Stat. Phys.* **117**, 975 (2004).
 - [4] R. Straube, M. J. Ward, and M. Falcke, *J. Stat. Phys.* **129**, 377 (2007).
 - [5] I. V. Grigoriev, Y. A. Makhnovskii, A. M. Berezhkovskii, and V. Y. Zitserman, *J. Chem. Phys.* **116**, 9574 (2002).
 - [6] D. Holcman and Z. Schuss, *J. Phys. A* **41**, 155001 (2008).
 - [7] A. Singer, Z. Schuss, and D. Holcman, *J. Stat. Phys.* **122**, 465 (2006).
 - [8] A. Singer, Z. Schuss, and D. Holcman, *J. Stat. Phys.* **122**, 491 (2006).
 - [9] A. Singer, Z. Schuss, D. Holcman, and R. S. Eisenberg, *J. Stat. Phys.* **122**, 437 (2006).
 - [10] A. Singer, Z. Schuss, and D. Holcman, *Phys. Rev. E* **78**, 051111 (2009).
 - [11] C. Chevalier, O. Benichou, B. Meyer, and R. Voituriez, *J. Phys. A* **44**, 025002 (2011).
 - [12] S. Pillay, M. J. Ward, A. Peirce, and T. Kolokolnikov, *Multiscale Model. Simul.* **8**, 803 (2010).
 - [13] A. F. Cheviakov, M. J. Ward, and R. Straube, *Multiscale Model. Simul.* **8**, 836 (2010).
 - [14] X. Chen and A. Friedman, *SIAM J. Math. Anal.* **43**, 2542.
 - [15] R. H. Hardin, N. J. A. Sloane, and W. D. Smith, <http://www.research.att.com/~njas/electrons/index.html>.
 - [16] T. Erber and G. M. Hockney, *J. Phys. A* **24**, 1369 (1991).
 - [17] E. A. Rakhmanov, E. B. Saff, and Y. M. Zhou, *Math. Res. Lett.* **1**, 647 (1994).

- [18] E. A. Rakhmanov, E. B. Saff, and Y. M. Zhou, in *Computational Methods and Function Theory 1994 (Penang)*, Ser. Approx. Compos. 5 (World Scientific, River's Edge, NJ, 1995), pp. 293–309.
- [19] B. Bergersen, D. Boal, and P. Palfy-Muhoray, *J. Phys. A* **27**, 2579 (1994).
- [20] C. B. Muratov and S. Y. Shvartsman, *Multiscale Model. Simul.* **7**, 44 (2008).
- [21] T. Kolokolnikov, M. Titcombe, and M. J. Ward, *Eur. J. Appl. Math.* **16**, 161 (2005).
- [22] T. Kolokolnikov, M. J. Ward, and J. Wei, *J. Nonlinear Sci.* **19**, 1 (2009).
- [23] J. D. Pintér, *Global Optimization in Action* (Kluwer Academic, Dordrecht, Netherlands, 1996).
- [24] J. D. Pintér, <http://plato.la.asu.edu/gom.html> (1996).
- [25] GANSO Software Library: University of Ballarat, Ballarat, Victoria, Australia, www.ballarat.edu.au/ciao.
- [26] M. C. Kropinski and B. Quaife, *J. Comput. Phys.* **230**, 425 (2010).